

Research Article

Bhawini Prasad*

Study of nanolayer on red blood cells as drug carrier in an artery with stenosis

<https://doi.org/10.1515/cmb-2023-0103>

received July 01, 2023; accepted September 22, 2023

Abstract: This article discusses a novel idea from cell therapy in which nanoparticles (NPs) are adsorbed on red blood cells (RBCs). RBCs serve as a drug carrier for NPs or nanodrugs adsorbed on the cell membrane of RBC. For the purpose of examination, Fe_3O_4 NPs are adsorbed on RBCs, collectively called NP-RBC complex. RBCs being a natural vascular carrier, have high transfusion rates and biocompatibility. This mathematical study provides a basis to attempt nanodrug delivery via RBCs, as carriers for nanodrugs, to the stenosed sites in an artery. The mathematical model is developed for an artery with stenosis and a catheter that regards the temperature and velocity of the NP-RBC complex. Catheter coated with the NP-RBC complex is inserted into the lumen of the stenosed artery. The mathematical problem is solved numerically using Bernstein polynomials. The physical features were discussed through graphs plotted using MATLAB. The influence of parameters such as volume fraction, radius of the NP-RBC complex in blood, and the thickness of the nanolayer on RBCs was studied. A noticeable outcome states that the nanolayer of optimum thickness about 50–40 nm is suitable for this purpose. Thus, this is an attempt to study the delivery of NPs adsorbed on the surface of RBCs to develop newfangled strategies in nanomedicine bearing high precision and efficiency.

Keywords: nanoparticles, nanolayer, Stenosis, Bernstein polynomials

MSC 2020: 35Q92, 92C45, 97M60, 35A24, 76D05

1 Introduction

Cardiovascular diseases are the major reason for reducing life expectancy globally. Cardiovascular diseases have resulted in 17.9 million deaths in 2019, which represents 32% of deaths occurring worldwide. They also accounted for 38% premature deaths or deaths below the age of 70 years in 2019. It is estimated that more than 23 million deaths will occur due to cardiovascular diseases annually, by 2030 [14].

Atherosclerosis is a highly occurring cardiovascular ailment. It is an inflammation in the artery that causes a progressive buildup of plaques in the lining of arterial wall. The arterial lumen narrows due to the development of plaques that obstruct the flow of blood; these depositions are called stenosis [12]. The development of stenosis at the wall of artery is accompanied by significant changes in blood flow. If not treated properly, it may develop into myocardial infarction because of plaque rupture with thrombus formation.

Catheters are a standard medical tool for the diagnosis and treatment of stenosis. They effectively clear the blockages in the artery and can also be used to monitor blood pressure and blood velocity. Introduction of a catheter, thus, alters the mechanics in the stenosed artery, and hence, it is an interesting area of mathematical investigation.

Despite the developments in medical and therapeutic management of cardiovascular diseases, the outcomes do not go very well with the treatments. This occurs owing to the lack of targeted theranostic.

* Corresponding author: Bhawini Prasad, Department of Mathematics, Harcourt Butler Technical University, Kanpur, Uttar Pradesh 208002, India, e-mail: jayabhawini@gmail.com

Biomedicine aims to continuously evolve and bring about improvements in the therapeutic index of the drug. The ability of any drug to survive in physiological environment determines the success of drug. Cell therapy using red blood cells (RBCs) is a novel method to answer the discrepancies of conventional methods [17]. Cell therapy offers advantages over conventional therapies because of better cellular networks. RBCs are the blood cells occurring in highest abundance, approximately $5 \times 10^{12}/L$, in the blood. Thus, they make about 45% of the total blood volume and hence are widely distributed throughout the circulation. The use of RBCs as drug carriers has been a keen area of research since the 1980s. The RBCs are biconcave disc-shaped without cell organelles that allow for high surface area in comparison with volume, which accredits to a higher loading of drugs. RBCs possess longevity in circulation, for instance, 45 days in mice and 120 days in humans. Thus, RBCs have possible use in vascular delivery of surface-bound drugs as carriers. Also, unlike other carriers, loading drug on RBCs does not interfere with the normal functioning of RBCs. But instead, the drugs can be released more conveniently [5]. Such extraordinary mechanical and structural characteristics of RBCs make them a remarkable agent for the delivery of drug.

The adsorption or assimilation of drugs on RBCs' membrane can prevent the phagocytosis of drugs and can also reduce their possible biotoxicity [16]. RBC membrane has a unique combination of mechanical flexibility to squeeze through microvessels and physical sturdiness to tolerate high stress conditions in circulation. Thus, RBCs are less fragile and more resistant cells. The RBC membrane renders a platform that encompasses the advantages of native RBCs and drugs. Coupling RBCs and drugs enables their transport in the vasculature without their untimely clearance. A number of studies over the past three decades have shown that encapsulating drugs on RBCs remarkably influences to improve the drug dynamics by prolonging their circulation in body [23]. Due to these likeable properties, the adsorption of drugs on RBCs is developing and progressing, in methodologies as well as experimentally, to aid in their clinical applications.

Cell therapy in combination with nanoparticles (NPs) is a new idea of drug delivery. RBCs are the most suitable carrier of NPs due to their enhanced compatibility in the system owing to their safe transfusion. The use of NPs in medicine holds promising advantages for the delivery of drugs at the specified site [10]. Loading of NPs on the RBCs has emerged as a promising strategy, because it was reported that when NPs alone were injected in the blood, they accumulated in liver or were cleared by macrophages [4]. Nanoformulations using RBCs increase the tolerability of drug in the immune system offering drug stability.

Pan et al. [17] studied the effect of NPs on the biocompatibility of RBCs as drug carrier. Their observation on mouse's RBCs stated that RBCs can house millions of the NPs per microlitres of blood. Pan et al. [16] studied the pharmacokinetics of the NP-RBC complex and proved its usefulness in drug delivery. Xia et al. [23] used RBC membrane-camouflaged NPs in the treatment of tumours.

In order to achieve the adsorption of nanolayer on RBCs, RBCs are first separated and collected from a blood sample. They are then washed with ice-cold water and dipped in a hypotonic solution containing the required NPs. NPs then adsorb on the surface of RBCs. This solution is centrifuged, and the supernatant is discarded. The process is repeated for a number of times depending on the nature of nanodrug. The drug so formed after nanolayer is adsorbed on RBCs is called the NP-RBC complex. NP-RBC complex can be administered into circulation in many ways. Here, it is considered that the complex is coated on the catheter and then inserted into the artery. These complexes imitate the movement of RBCs' in the blood and thus can reach the desired site.

NPs are loaded on the RBCs and then inoculated back into circulation via coating on the catheter [21]. These therapeutics using RBCs as nanocarriers promote guided, sustained, and selective drug release to the diseased site whilst maintaining the homogeneous distribution of drug. To achieve the purpose, various kinds of inorganic NPs such as Fe_3O_4 , Si, and Au are used. Fe_3O_4 NPs have proven to possess excellent targeting ability after their coating on the surface of RBC. Rao et al. [20] had designed Fe_3O_4 NPs coated on RBCs that exhibited superior biocompatibility and degradability.

Once the NPs reach the blood-stream, it is important to assess their behaviour. Nanofluids are nanomaterials dispersed in a base fluid such as water and organic solvents [19]. Nanofluids display anomalous thermal properties and thus have gained significant interest over the last 10 years [9]. The two factors responsible for this are surface area and quantum effects. As the size of particle reaches the nanoscale, the nanofluids display

different thermal properties. It has been shown that small amounts of nanosized materials in a fluid enhance its thermal conductivity, thermal expansion, and viscosity to a large extent. The NP-RBC complex in blood is treated as nanofluid and the traits of which have been discussed applying the thermal properties of nanofluid.

Furthermore, the mathematical solution to the problem has been found using Bernstein polynomials. Bernstein polynomials solve differential equations approximately [2,6]. These positive polynomials are defined on the interval such that their sum is always unity. This method reduces the mathematical model into a set of algebraic equations that reduces the complexity.

Based on the aforementioned literature survey, a mathematical model to analyse cell therapy via the deposition of NPs on RBCs has not been conducted so far. In this mathematical study, the NPs coated on RBCs, collectively identified as the NP-RBC complex, are coated on the catheter, which is inserted in the lumen of the artery. The continuity equation, Navier-Stokes equation for fluid flow, and temperature diffusion equation are used to design the mathematical model. Thermophysical properties such as viscosity, thermal conductivity, and thermal expansion have been considered. Bernstein polynomials are used to solve the problem. The temperature and velocity of NP-RBC in the blood have been found and investigated by plotting graphs. The influence of volume fraction of the NP-RBC complex and thickness of the NP layer on RBC has been monitored graphically using MATLAB. The aforementioned model has probable applications for the treatment of cardiovascular diseases using targeted drug delivery.

2 Formulation of the model

The geometrical representation of the mathematical model of a catheterized artery with stenosis is shown in Figure 1. The flow is described [3] by cylindrical co-ordinates (r', θ', z') .

The geometry of stenosis is

$$R'(z') = \begin{cases} R_0 - \frac{2\delta'}{L'_0}(z' - d'); & d' \leq z' \leq d' + \frac{L'_0}{2}, \\ R_0 - \frac{\delta'}{2} \left[1 + \cos \frac{2\pi}{L'_0} \left(z' - d' - \frac{L'_0}{2} \right) \right]; & d' + \frac{L'_0}{2} \leq z' \leq d' + L'_0, \\ R_0, & \text{otherwise.} \end{cases} \quad (1)$$

The equations governing the motion are as follows:

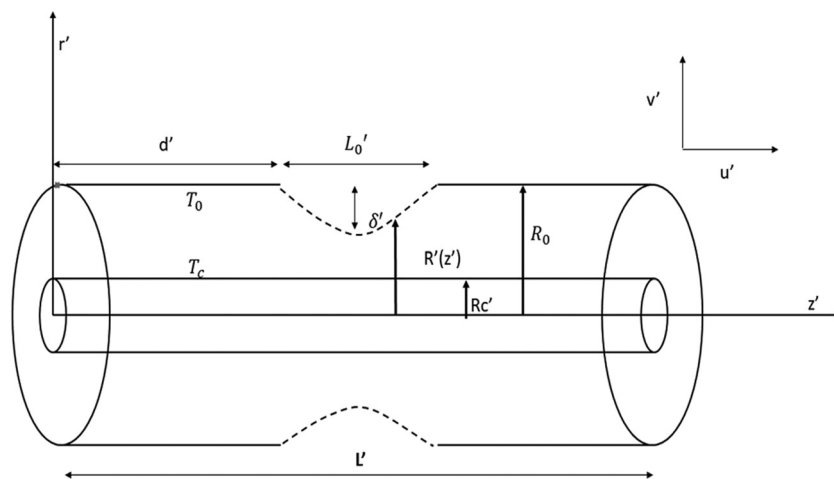


Figure 1: Geometrical representation.

Continuity equation:

$$\frac{\partial \rho_{nf}}{\partial t'} + \frac{1}{r'} \frac{\partial(r\rho_{nf}v')}{\partial r'} + \frac{1}{r'} \frac{\partial \rho_{nf}w'}{\partial \theta'} + \frac{\partial \rho_{nf}u'}{\partial z'} = 0. \quad (2)$$

Navier-Stokes equation:

$$\frac{\partial v'}{\partial t'} + v' \frac{\partial v'}{\partial r'} + \frac{u'}{r'} \frac{\partial v'}{\partial \theta'} - \frac{u'^2}{r'} + u' \frac{\partial v'}{\partial z'} = F_{r'} - \frac{1}{\rho_{nf}} \frac{\partial p'}{\partial r'} + \frac{\mu_{nf}}{\rho_{nf}} \left(-\frac{v'}{r^2} + \frac{1}{r'} \frac{\partial}{\partial r'} \left(r' \frac{\partial v'}{\partial r'} \right) + \frac{1}{r'^2} \frac{\partial^2 v'}{\partial \theta'^2} + \frac{\partial^2 v'}{\partial z'^2} \right. \\ \left. - \frac{2}{r'^2} \frac{\partial w'}{\partial \theta'} \right), \quad (3)$$

$$\frac{\partial w'}{\partial t'} + v' \frac{\partial w'}{\partial r'} + \frac{u'}{r'} \frac{\partial w'}{\partial \theta'} - \frac{v' w'}{r'} + u' \frac{\partial w'}{\partial z'} = F_{\theta'} - \frac{1}{\rho_{nf}} \frac{\partial p'}{\partial \theta'} + \frac{\mu_{nf}}{\rho_{nf}} \left(-\frac{w'}{r^2} + \frac{1}{r'} \frac{\partial}{\partial r'} \left(r' \frac{\partial w'}{\partial r'} \right) + \frac{1}{r'^2} \frac{\partial^2 w'}{\partial \theta'^2} \right. \\ \left. + \frac{\partial^2 w'}{\partial z'^2} + \frac{2}{r'^2} \frac{\partial v'}{\partial \theta'} \right), \quad (4)$$

$$\frac{\partial u'}{\partial t'} + v' \frac{\partial u'}{\partial r'} + \frac{u'}{r'} \frac{\partial u'}{\partial \theta'} + u' \frac{\partial u'}{\partial z'} = F_{z'} - \frac{1}{\rho_{nf}} \frac{\partial p'}{\partial z'} + \frac{1}{\rho_{nf}} \left(\frac{1}{r'} \frac{\partial}{\partial r'} \left(r' \frac{\partial u'}{\partial r'} \right) + \frac{1}{r'^2} \frac{\partial^2 u'}{\partial \theta'^2} + \frac{\partial^2 u'}{\partial z'^2} \right), \quad (5)$$

where F' is the body forces in various indices, μ_{nf} is the viscosity, and ρ_{nf} is the nanofluid density.

Temperature diffusion equation:

$$\frac{1}{D_{nf}} \frac{\partial T'}{\partial t'} = \frac{\partial^2 T'}{\partial r'^2} + \frac{1}{r'} \frac{\partial T'}{\partial r'} + \frac{1}{r'^2} \frac{\partial^2 T'}{\partial \theta'^2} + \frac{\partial^2 T'}{\partial z'^2} + \frac{H}{k_{nf}}, \quad (6)$$

where D_{nf} is the thermal diffusivity, k_{nf} is the nanofluid thermal conductivity, and H is the constant heat absorption or generation parameter.

Equations (1)–(6) assume the following considerations:

- (1) Flow is two-dimensional and axisymmetric.
- (2) Flow is steady, laminar, and incompressible.
- (3) The insertion of catheter considers constant heat generation/absorption.

Now, the equation of continuity

$$\frac{\partial u'}{\partial z'} = 0. \quad (7)$$

The Navier-Stokes equation and its boundary conditions

$$-\frac{\partial P'}{\partial z'} - \frac{1}{r'} \frac{\partial}{\partial r'} (r' \mu_{nf}) + g(\rho \gamma)_{nf} (T' - T_0) = 0, \quad (8)$$

where γ_{nf} is the thermal expansion of the NP-RBC complex.

No slip condition is assumed at the catheter:

$$u' = 0 \text{ at } r' = R_c \quad (9)$$

At the boundary of artery, Darcy's law is applied as the NP-RBC complex shall be absorbed at the stenosed site:

$$u' = u'_{B} \text{ at } r' = R'(z'), \quad (10)$$

$$\frac{\partial u'}{\partial r'} = \frac{\sigma'}{\sqrt{Da}} (u'_{B} - u'_{p}) \text{ at } r' = R'(z'), \quad (11)$$

in which

$$u'_{p} = -\frac{Da}{\mu_{nf}} \frac{\partial p'}{\partial z'} \text{ is the velocity at permeable boundary,} \quad (12)$$

where u'_B is the velocity of slip, σ' is the parameter of slip, and Da is the Darcy number.

The temperature diffusion equation and conditions at boundary are as follows:

$$\frac{\partial^2 T'}{\partial r'^2} + \frac{1}{r'} \frac{\partial T'}{\partial r'} + \frac{H}{k_{nf}} = 0. \quad (13)$$

The temperature at the surface of artery is T_0 and on the surface of the catheter T_c :

$$T' = T_0 \text{ at } r' = R'(z'), \quad (14)$$

$$T' = T_c \text{ at } r' = R'_c. \quad (15)$$

As described earlier, the nanofluids display enhanced thermal properties such as thermal conductivity and viscosity. Over the time, many studies have described various ideas to comprehend the properties of nanofluids. The prime model in this regard for nanofluid thermal conductivity was given by Maxwell [11]. Yu and Choi [24] reformed this model by allowing for the traits of nanolayer on the membrane of dispersed particles, described mathematically as:

$$\frac{k_{nf}}{k_f} = \frac{k_p + 2k_f + 2\phi(k_p - k_f)(1 + \beta)^3\phi}{k_p + 2k_f - \phi(k_p - k_f)(1 + \beta)^3\phi}, \quad (16)$$

where $\beta = \frac{d_{nl}}{2r_p}$, d_{nl} is the thickness of nanolayer, r_p is the radius of NP-RBC complex, k_f is the thermal conductivity of the base fluid, k_p is the thermal conductivity of the NP-RBC complex, and ϕ is the volume fraction of the NP-RBC complex in blood.

Viscosity of nanofluid is another important property that directly affects the motion of the NP-RBC complex. The classical model for viscosity of nanofluid was given by Einstein [7]. Hosseini et al. [8] gave a more advanced model for predicting the viscosity in the presence of nanolayer. This model holds consistency to experimental verifications on water-based nanofluids:

$$\frac{\mu_{nf}}{\mu_f} = \exp\left(a + c_1 T' + c_2 \phi + c_3 \left(\frac{r_p}{1 + d_{nl}}\right)\right), \quad (17)$$

where T' is the temperature, and a , c_1 , c_2 , and c_3 are the empirical constants.

The principle of conservation of mass gives the density of nanofluid as follows:

$$\rho_{nf} = (1 - \phi)\rho_f + \phi\rho_p, \quad (18)$$

where ρ_f is the density of blood and ρ_p is the density of the NP-RBC complex.

Thus, the thermal expansion of nanofluid $(\rho\gamma)_{nf}$ is expressed as:

$$(\rho\gamma)_{nf} = (1 - \phi)(\rho\gamma)_f + \phi(\rho\gamma)_p, \quad (19)$$

where γ_f is the thermal expansion of blood and γ_p is the thermal expansion of the NP-RBC complex.

The scheme for non-dimensionalization is as follows:

$$\begin{aligned} z' &= \frac{z'}{R_0}, & u &= \frac{u'}{u_o}, & P &= \frac{P'}{\rho_f u_o^2}, & \text{Re} &= \frac{R_o u_o \rho_f}{\mu_f}, & \text{Da} &= \frac{k_f}{R_0^2}, \\ \theta &= \frac{T' - T_0}{T_c - T_0}, & \text{Gr} &= \frac{g(\rho\gamma)_f R_0^2 (T_c - T_0)}{u_o \mu_f}, & h &= \frac{H R_0^2}{(T_c - T_0) k_f}, & r &= \frac{r'}{R_0}, \end{aligned} \quad (20)$$

where u_o is the reference velocity, Re is the Reynolds number, Da is the Darcy number, Gr is the Grashof number, and h is the heat source parameter.

The final equations after non-dimensionalizing the geometry of stenosis, Navier-Stokes equation, temperature diffusion, and respective boundary conditions are given as follows:

$$R(z) \begin{cases} 1 - \frac{2\delta}{L_0}(z - d); & d \leq z \leq d + \frac{L_0}{2}, \\ 1 - \frac{\delta}{2} \left[1 + \cos \frac{2\pi}{L_0} \left(z - d - \frac{L_0}{2} \right) \right]; & d + \frac{L_0}{2} \leq z \leq d + L_0, \\ 1, \text{ otherwise} \end{cases} \quad (21)$$

$$-\operatorname{Re} \frac{\partial P}{\partial z} + \mu_f \exp \left[a + c_1 \theta \left(\frac{T_c}{T_0} - 1 \right) + c_2 \phi + c_3 \left(\frac{r_p}{1 + d_{nl}} \right) \right] \frac{\partial}{\partial r} \left(r \frac{\partial u}{\partial r} \right) + \left((1 - \phi) + \phi \frac{(\rho\gamma)_p}{(\rho\gamma)_f} \right) Gr\theta = 0, \quad (22)$$

$$\frac{\partial^2 \theta}{\partial r^2} + \frac{1}{r} \frac{\partial \theta}{\partial r} + h \left[\frac{k_p + 2k_f + 2\phi(k_p - k_f)\phi(1 + \beta)^3}{k_p + 2k_f - \phi(k_p - k_f)\phi(1 + \beta)^3} \right] = 0, \quad (23)$$

$$u = 0 \text{ at } r = Rc, \quad (24)$$

$$u = u_B \text{ at } r = R(z), \quad (25)$$

$$\frac{\partial u}{\partial r} = \frac{\sigma}{\sqrt{Da}} (u_B - u_p) \text{ at } r = R(z), \quad (26)$$

where

$$u_p = -\frac{Da}{\mu_f} \frac{\partial p}{\partial z} \text{ at } r = R(z), \quad (27)$$

$$\theta = 0 \text{ at } r = R(z), \quad (28)$$

$$\theta = 1 \text{ at } r = Rc. \quad (29)$$

3 Solution

The solution to equations (22) and (23) using the boundary conditions (24) to (29) is found numerically using Bernstein polynomials. Bernstein polynomials are defined as basis functions in the Hilbert space L_2 [0,1] expressed as:

$$B_{k,m}(r) = \binom{m}{k} r^k (1 - r)^{m-k}, \quad k = 0, 1, 2, \dots, m, r \in [0, 1], \quad (30)$$

where

$$\binom{m}{k} = \frac{m!}{k!(m - k)!}. \quad (31)$$

Thus, we write a polynomial $u_m(r)$ of degree m as Bernstein polynomial $B_{k,m}(r)$ as:

$$u_m(r) = \sum_{k=0}^m c_{1,k} B_{k,m}(r), \quad (32)$$

where $c_{1,k}$ are the constants.

Now, finding the s -order differential with respect to r of the polynomial $u_m(r)$

$$\frac{d^s u_m(r)}{dr^s} = \frac{d^s}{dr^s} \left(\sum_{k=0}^m c_{1,k} B_{k,m}(r) \right), \quad (33)$$

$$\frac{d^s u_m(r)}{dr^s} = \sum_{k=0}^m c_{1,k} \frac{d^s}{dr^s} B_{k,m}(r). \quad (34)$$

Now,

$$\frac{d^s}{dr^s} B_{k,m}(r) = \sum_{i=s-k}^{m-k} \binom{m}{k} \binom{m-k}{i} (-1)^k \frac{\Gamma(k+i+1)}{\Gamma(k+i+1-s)} r^{k+i-s} \quad k+i-s > 0. \quad (35)$$

Thus,

$$\frac{d^s u_m(r)}{dr^s} = \sum_{k=0}^m c_{1,k} \sum_{i=s-k}^{m-k} \binom{m}{k} \binom{m-k}{i} (-1)^k \frac{\Gamma(k+i+1)}{\Gamma(k+i+1-s)} r^{k+i-s}. \quad (36)$$

Now, after allocating r_j , $j = 0, 1, \dots, m-2$, and z_l , $l = 0, 1, \dots, q$ for framing our equations and boundary conditions in terms of Bernstein polynomials, we obtain

$$\begin{cases} -\operatorname{Re} \frac{\partial P}{\partial z} + \mu_f \exp \left(a + c_1 \theta_j \left(\frac{T_c}{T_0} - 1 \right) + c_2 \phi + c_3 \left(\frac{r_p}{1 + d_{nl}} \right) \right) \\ \frac{\partial}{\partial r_j} \left(r_j \sum_{k=0}^m c_{1,k} \sum_{i=1-k}^{m-k} \binom{m}{k} \binom{m-k}{i} (-1)^k \frac{\Gamma(k+i+1)}{\Gamma(k+i)} r^{k+i-1} \right) + \left((1-\phi) + \phi \frac{(\rho\gamma)_p}{(\rho\gamma)_f} \right) G r \theta_j = 0, \end{cases} \quad (37)$$

$$\begin{cases} \sum_{k=0}^m c_{2,k} \sum_{i=2-k}^{m-k} \binom{m}{k} \binom{m-k}{i} (-1)^k \frac{\Gamma(k+i+1)}{\Gamma(k+i-1)} r^{k+i-2} \\ + \frac{1}{r_j} \left(\sum_{k=0}^m c_{2,k} \sum_{i=1-k}^{m-k} \binom{m}{k} \binom{m-k}{i} (-1)^k \frac{\Gamma(k+i+1)}{\Gamma(k+i)} r^{k+i-1} \right) + h \left[\frac{k_p + 2k_f + 2\phi(k_p - k_f)\phi(1+\beta)^3}{k_p + 2k_f - \phi(k_p - k_f)\phi(1+\beta)^3} \right] = 0, \end{cases} \quad (38)$$

$$\sum_{k=0}^m c_{1,k} B_{k,m}(r) = 0 \text{ at } r_j = R_c, \quad (39)$$

$$\sum_{k=0}^m c_{1,k} B_{k,m}(r) = u_B \text{ at } r_j = R(z_l), \quad (40)$$

$$\sum_{k=0}^m c_{1,k} B_{k,m}(r) = \frac{\alpha}{\sqrt{Da}} (u_B - u_p) \text{ at } r_j = R(z_l), \quad (41)$$

$$\sum_{k=0}^m c_{2,k} B_{k,m}(r) = 0 \text{ at } r_j = R(z_l), \quad (42)$$

$$\sum_{k=0}^m c_{2,k} B_{k,m}(r) = 1 \text{ at } r_j = R_c \quad (43)$$

Now, the solution to these algebraic equations is found using Gauss elimination method, in MATLAB.

4 Graphical results and discussions

RBCs are profusely occurring blood cells circulating in the body. Thus, they can be used on drug delivery system with certain modifications. Camouflaging the membrane of RBC to adsorb NPs as layer renders a platform that clubs the advantage of NPs with RBC, thus achieving enhanced biocompatibility and bioavailability. The changes in the pharmacokinetics when this NP-RBC complex enters the blood circulation via intravenous injection is the major concern of this study. The mathematical model is framed for an artery with stenosis. A catheter coated with Fe_3O_4 NP-RBC complex is inserted into the lumen of the artery. The model uses the continuity equation, the Navier-Stokes equation for fluid flow, and the temperature diffusion equations to describe the characteristics of the NP-RBC complex in blood. The temperature and velocity of the resultant nanofluid is found numerically using Bernstein polynomial approximations. The graphical analysis is performed using MATLAB. The effect of temperature of nanofluid θ is examined on different values of

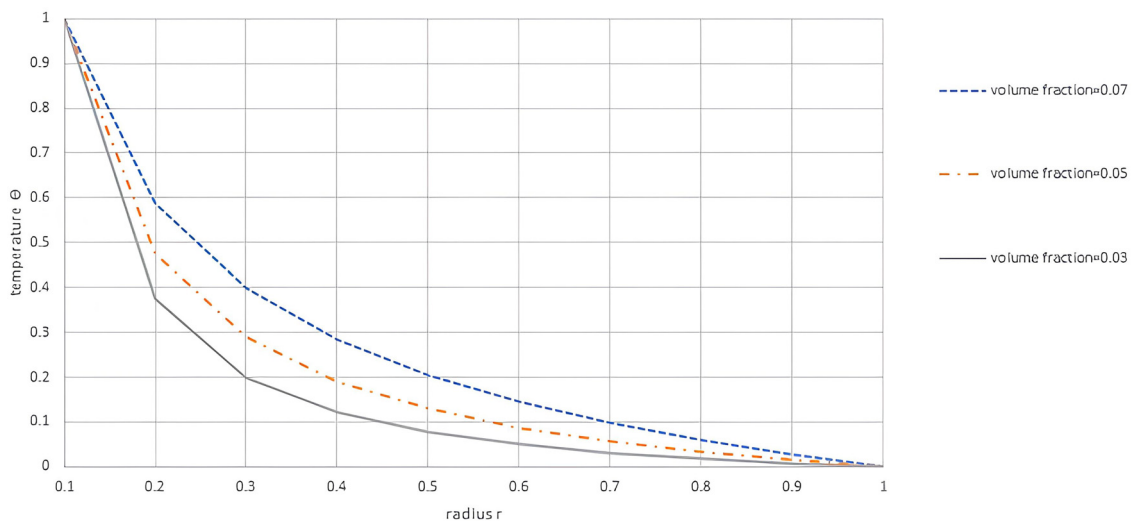


Figure 2: Behaviour of temperature θ of NP-RBC complex in blood against radial direction r with respect to volume fraction Θ .

volume fraction ϕ of the NP-RBC complex, radius r_p of the NP-RBC complex, thickness of nanolayer d_{nl} , and heat source parameter h , against radial direction r (Figures 2–5), while the effect of velocity u of nanofluid is observed on different values of volume fraction ϕ of the NP-RBC complex, radius r_p of the NP-RBC complex, thickness of nanolayer d_{nl} , stenosis depth δ , and Darcy number Da against radial direction r (Figures 6–10). The results are discussed in detail henceforth that have shown a good agreement with the existing literature. Table 1 lists the values of thermophysical quantities used at 300 K.

The trend of temperature θ against radial direction r with respect to the volume fraction ϕ of the NP-RBC complex in blood (Figure 2) shows that the temperature rises for an increase in volume fraction. Volume fraction is the representative of the number of solute particles in a solvent. Thus, an increase in the number of solute particles enhances the net Brownian motion that brings about an increase in temperature. Kumar et al. [9] reported a similar conclusion in their study of nanofluids. Also, this aspect of volume fraction is important to decide the amount of dosage that should be administered.

The graph of temperature θ against radial direction r with respect to the radius r_p of the NP-RBC complex (Figure 3) displays a rise in temperature for an enhancement in radius of the NP-RBC complex. This happens

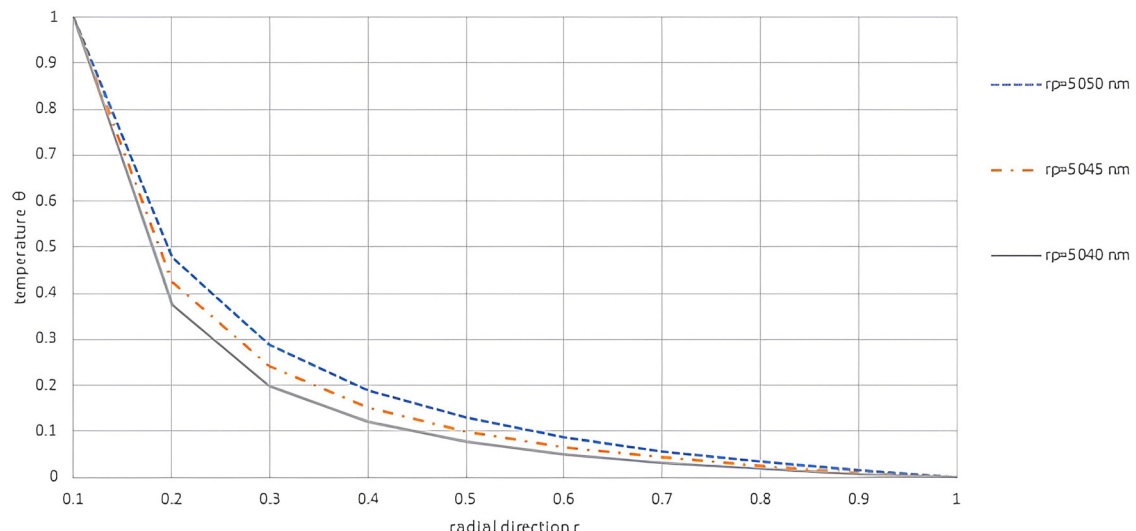


Figure 3: Behaviour of temperature θ of the NP-RBC complex in blood against radial direction r with respect to radius of NP-RBC complex r_p .

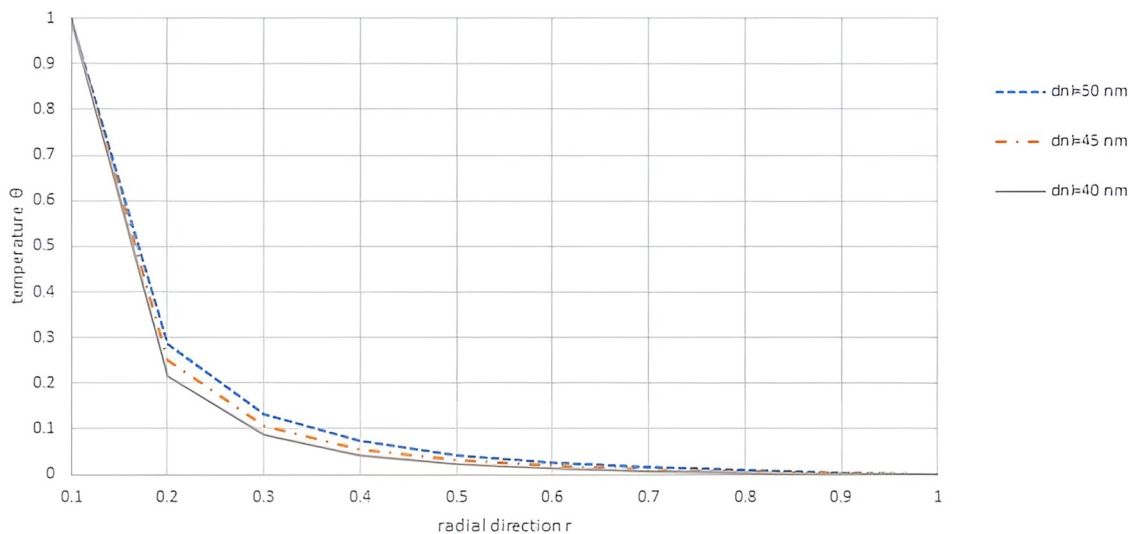


Figure 4: Behaviour of temperature θ of the NP-RBC complex in blood against radial direction r with respect to thickness of nanolayer d_{nl} .

because of the reduction in interparticle distance, which causes the temperature to rise because of increased Brownian motion. Wang et al. [22] in their study of shear kinetics of such complexes concluded that an average size of about 5,045 nm of the NP-RBC complex is apt for the drug delivery.

Similarly, the graph of temperature θ against radial direction r with respect to the thickness d_{nl} of nanolayer (Figure 4) displays a rise in temperature for an increased thickness. The reason is the same as above. Ajdnik et al. [1] in their experimental study of use of nanolayers for medicine gave homogenous observations. Gradually, under the effect of varying shear stress, the nanodrug shall be released upon entering the capillaries [22].

The temperature θ profile against radial direction r with respect to heat source parameter h (Figure 5) depicts that as the temperature increases for an increase in heat source parameter. Heat source parameter typifies the amount of heat generated or absorbed due to the insertion of catheter. Thus, there is a greater heat generation for an increased heat source parameter. This factor shall determine the optimum temperature of nanodrug to function.

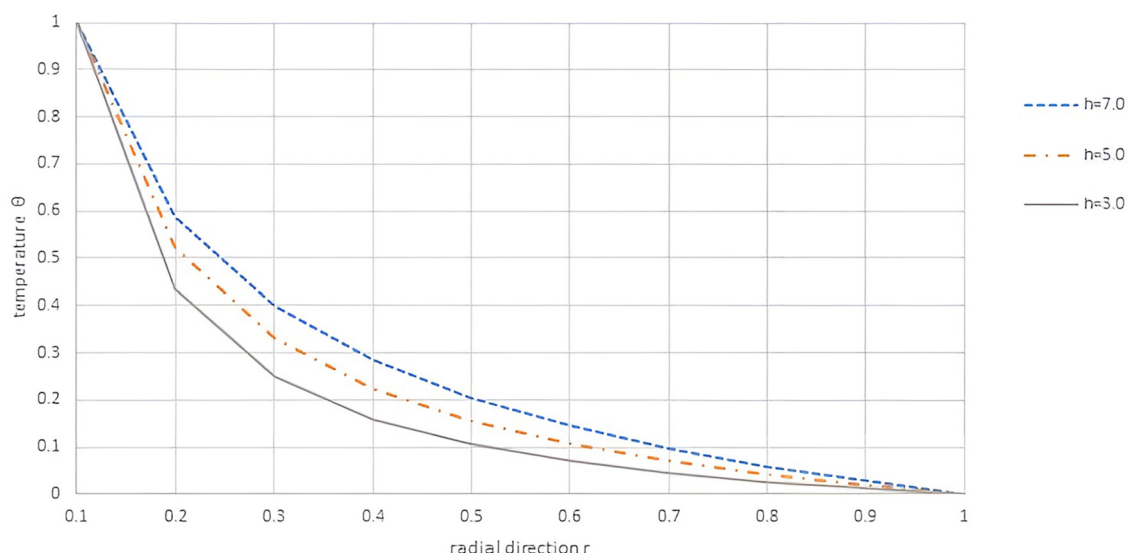
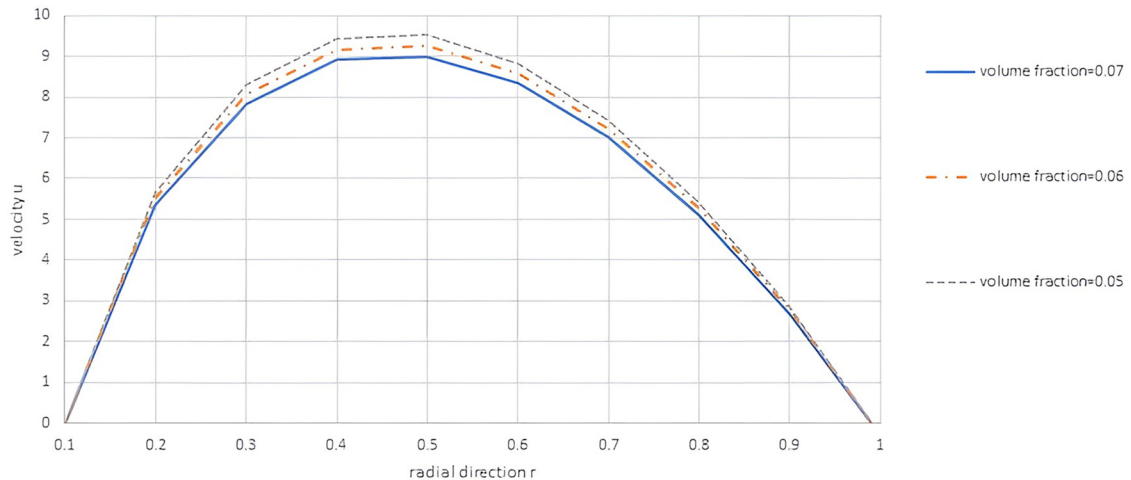


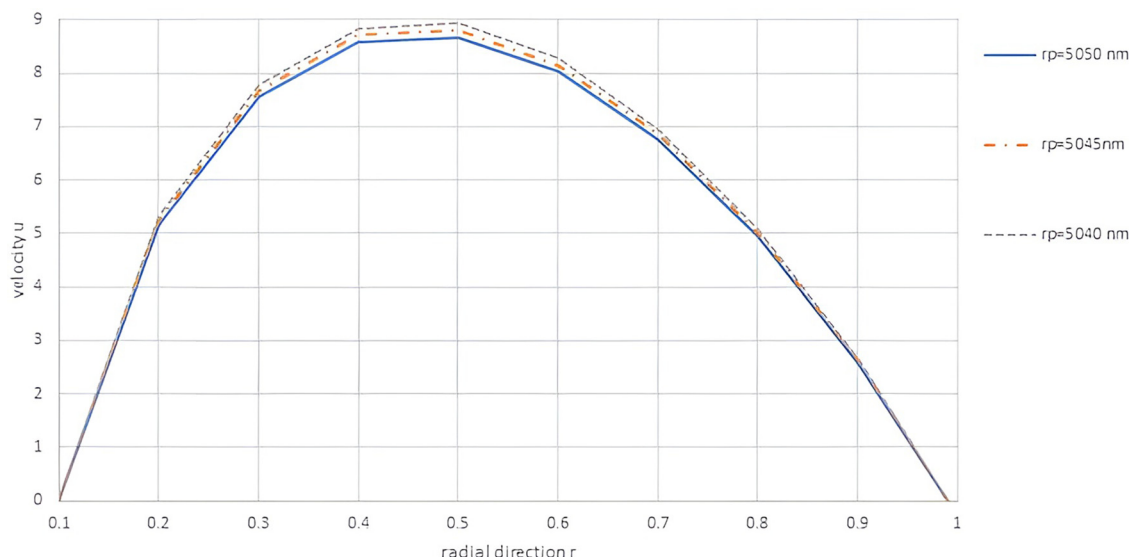
Figure 5: Behaviour of temperature θ of the NP-RBC complex in blood against radial direction r with respect to heat source parameter h .

Table 1: The values of thermophysical quantities of blood and nanoparticle used for calculations

Thermophysical quantities	Blood [18]	Fe_3O_4 NP [15]
Thermal conductivity	$0.49 \text{ W m}^{-1} \text{ K}^{-1} (k_f)$	$80.4 \text{ W m}^{-1} \text{ K}^{-1}$
Density	$1.093 \times 10^3 \text{ kg/m}^3 (\rho_f)$	$5,180 \text{ kg/m}^3$
Thermal expansion	$273.0003 \text{ K}^{-1} (\gamma_f)$	$273.150016 \text{ K}^{-1}$
Viscosity	4.5 cP	1.7 cP

**Figure 6:** Behaviour of velocity u of the NP-RBC complex in blood against radial direction r with respect to volume fraction Θ .

The trend of velocity u against radial direction r with respect to the volume fraction ϕ of the NP-RBC complex in blood (Figure 6) shows that velocity reduces for the rise in volume fraction. Since volume fraction is representative of the number of NP-RBC particles in blood, the increase in its value causes the viscous drag to increase because of an increase in Brownian motion, which decreases the net movement. Thus, the velocity decreases. Kumar et al. [9] also came up with the same conclusions. Hence, volume fraction physically regulates the drug dosage variability, working on the type of ailment.

**Figure 7:** Behaviour of velocity u of the NP-RBC complex in blood against radial direction r with respect to radius of NP-RBC complex rp .

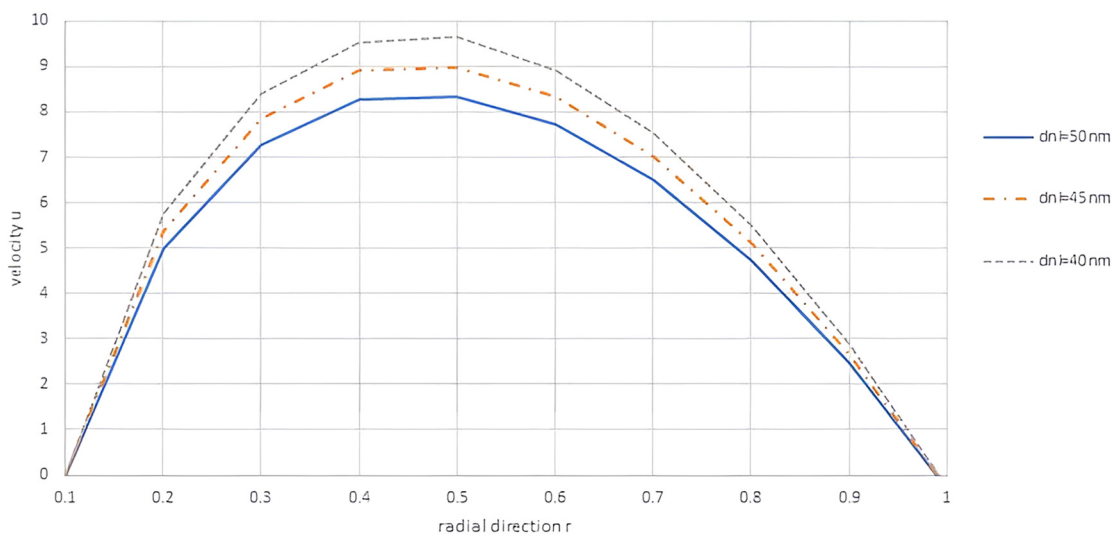


Figure 8: Behaviour of velocity u of the NP-RBC complex in blood against radial direction r with respect to thickness of nanolayer d_{nl} .

The profile of velocity u versus radial direction r with respect to radius r_p of the NP-RBC complex (Figure 7) shows that the velocity declines for an increase in radius. With the increase in radius, the interparticle distance decreases that results in increasing the random Brownian motion. Thus, the flow slows down. Wang et al. [22] also probed into similar kinetic details, experimentally.

The profile of velocity u versus radial direction r with respect to thickness d_{nl} of nanolayer (Figure 8) shows a decline in velocity for greater thickness. Similar reason as earlier can be attributed to the behaviour of velocity. Identical results were reported by Ajdnik et al. [1] to develop nanomedicines. Also, Brenner et al. [5] proclaimed the usefulness of nanolayer and NP-RBC complex with alike analysis.

The trend in velocity u against radial direction r with respect to stenosis depth δ (Figure 9) shows an increment in velocity with greater stenosis depth. Greater stenosis depth means lesser cross-sectional area of the artery available for blood flow. Thus, the velocity rises in a smaller cross-sectional area owing to Bernoulli's principle. Xia et al. [23] also established that the shape of tumour or stenosis is important to design the characteristics of the NP-RBC complex.

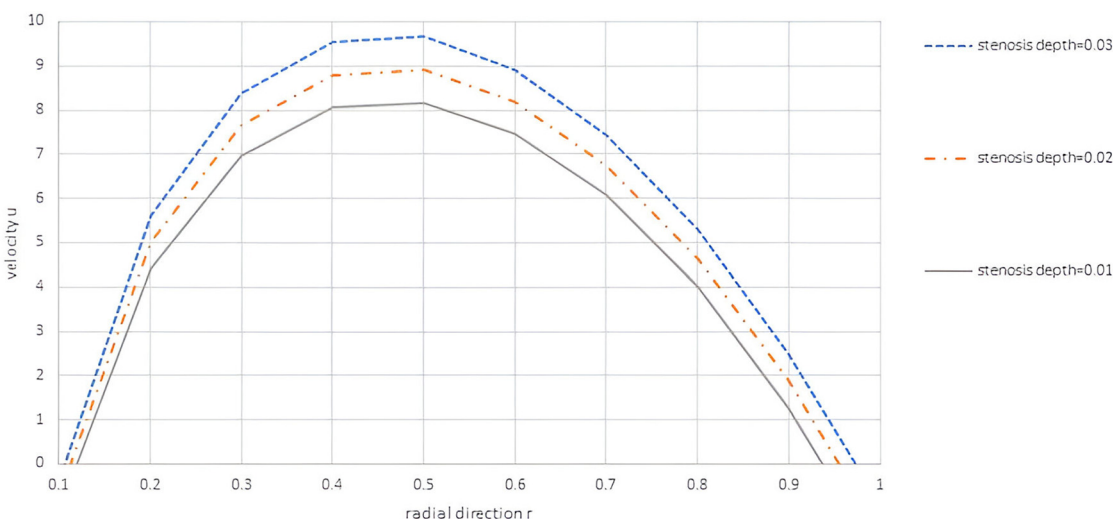


Figure 9: Behaviour of velocity u of the NP-RBC complex in blood against radial direction r with respect to stenosis depth δ .

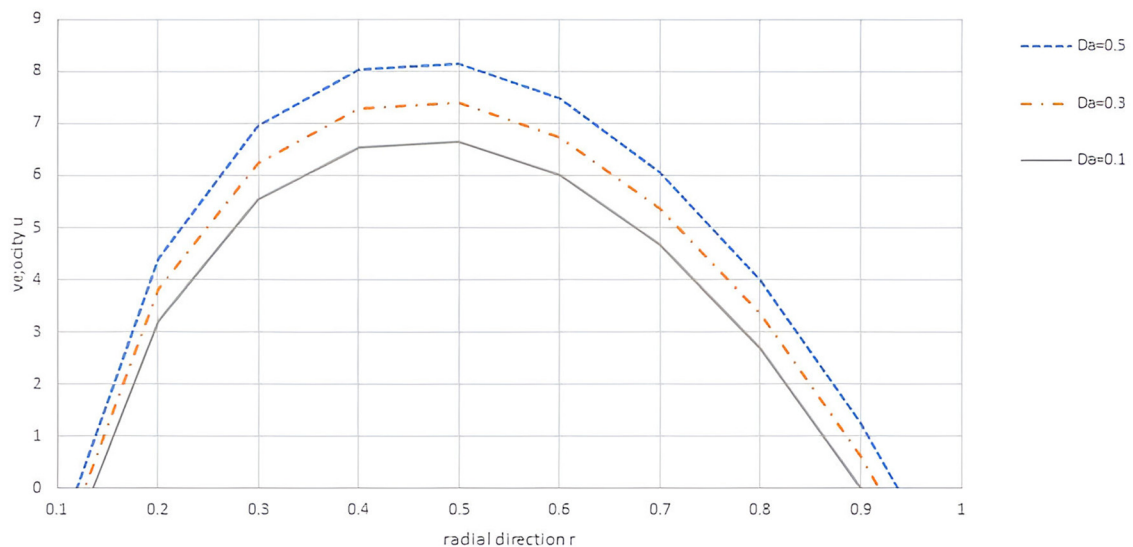


Figure 10: Behaviour of velocity u of the NP-RBC complex in blood against radial direction with respect to the Darcy number Da .

The trend in velocity u against radial direction r with respect to the Darcy number (Figure 10) shows that velocity rises for increased Darcy number Da . The Darcy number quantifies the effect of medium's permeability against the area of flow. The rise in the Darcy number enhances the convections on the medium due to higher permeability. Thus, the velocity rises. Moitioi and Shaw [13] also showed that the Darcy number boosted the drug targeting efficiency at the diseased site. The Darcy number controls the amount of drug transferred and absorbed by the diseased cells, thus eventually help in developing targeted theranostic.

5 Conclusion

Drug delivery via NPs has aroused as the latest and highly effective therapeutic technique in the treatment of cardiovascular diseases. The nanodrugs are targeted at the diseased site and accumulated there. This increases their retention at the site, reduces dosage, and also avoids side effects. However, the rapid clearance of nanodrugs because of phagocytosis reduces the effectiveness of the drug.

Blood cells have provided a new avenue for drug delivery. RBCs occur in the highest number in blood; thus, they provide a suitable platform for drug loading. Loading NPs on blood cells such as RBCs increases the circulation time of nanodrugs. These benefits have leveraged the use of NP-RBC complex in delivery of drug for the treatment of cardiovascular diseases such as atherosclerosis.

In the current mathematical study, Fe_3O_4 NP-RBC complex is coated on the catheter that is inserted into the lumen of the stenosed artery. The results have been found for temperature and velocity of NP-RBC. The findings can be summarized as:

- (1) The temperature of the NP-RBC complex in blood increases for an increase in volume fraction ϕ of the NP-RBC complex, radius r_p of the NP-RBC complex, thickness of nanolayer d_{nl} , and heat source parameter h .
- (2) The velocity of the NP-RBC complex in blood decreases for an increase in volume fraction ϕ of the NP-RBC complex, radius r_p of the NP-RBC complex, and thickness of nanolayer d_{nl} .
- (3) The velocity of the NP-RBC complex in blood increases for an increase in values of stenosis depth δ and the Darcy number Da .

The NP-RBC-derived complex has been found to be beneficial in many respects such as immune-compatibility and controlled drug release. Certain aspects such as removal of these complexes and cost-effective

production need to be still explored and taken care of. Addressing these challenges holds great potential for nanodrug delivery using RBCs.

Funding information: This research received no specific grant from any funding agency, commercial, or non-profit sectors.

Conflict of interest: The author have no conflicts of interest to disclose.

Ethical approval: This research did not require ethical approval.

Data availability statement: Data sharing is not applicable to this article as no new data were created or analyzed in this study.

References

- [1] Ajdnik, U., Zemljic, L. F., Plohl, O., Perez, L., Trcek, J., Bracic, M., & Mohan, T. (2021). Bioactive functional nanolayers of Chitosan-Lysine Surfactant with single and mixed protein repellent and antibiofilm properties for medical implants. *Applied Materials and Interfaces*, 13, 23352–23368.
- [2] Bataineh, A. S., Isik, O. R., & Hashim, I. (2016). Bernstein method for the MHD flow and heat transfer of a second grade fluid in a channel with porous wall. *Alexandria Engineering Journal*, 55, 2149–2156. <https://dx.doi.org/10.1016/j.aej.2016.06.022>.
- [3] Bird, R. B., Stewart, W. E., & Lightfoot, E. N. *Transport phenomena*. ISBN-13:978-0470115398.
- [4] Brenner, J., Mitragotri, S., & Muzykantov, V. (2021). Red blood cell Hitchhiking: A novel approach for vascular delivery of nanocarriers. *Annual Reviews in Biomedical Engineering*, 13, 23, 225–248. <https://doi.org/10.1146/annurev-bioeng-121219-024239>.
- [5] Brenner, J. S., Pan, D. C., Myerson, J. W., & Contreras, O. A. M. (2018). Red blood cell-hitchhiking boosts delivery of nanocarriers to chosen organs by orders of magnitude. *Nature Communications*, 9, 2684. <https://doi.org/10.1038/s41467-018-05079-7>.
- [6] Chatterjee, A., Changdar, S., & De, S. (2020). Study of nanoparticle as a drug carrier through stenosed arteries using Bernstein polynomials. *International Journal for Computational Methods in Engineering Science and Mechanics*, 21(5), 243–251. <https://doi.org/10.1080/15502287.2020.1821125>.
- [7] Einstein, A. (1906). Eine neue bestimmung der molekuldimensionen. *Annals of Physics*, 19, 289–306.
- [8] Hosseini, S. M., Moghadassi, A. R., & Henneke, D. E. (2010). A new dimensionless group model for determining the viscosity of nanofluids. *Journal of Thermal Analysis in Calorimetry*, 100, 873–877. <https://dx.doi.org/10.1007/s10973-010-0721-0>.
- [9] Kumar, N. N., Sastry, D. R. V. S. R. K., & Shaw, S. (2022). Irreversibility analysis of an unsteady micropolar CNT-blood nanofluid flow through a squeezing channel with activation energy-application in drug delivery. *Computer Methods and Programs in Biomedicine*, 226, 107156. <https://doi.org/10.1016/j.cmpb.2022.107156>.
- [10] Le, Q., Lee, J., Lee, H., Shim, G., & Oh, Y. (2021). Cell membrane-derived vesicles for delivery of therapeutic agents. *Acta Pharmaceutica Sinica B*, 11(8), 2096–2113.
- [11] Maxwell, J. C. (1873). *A treatise on electricity and magnetism*. Oxford: Clarendon Press.
- [12] Mishra, S., Siddiqui, S. U., & Medhavi, A. (2011). Blood flow through a composite stenosis in an artery with permeable wall. *Applications and Applied Mathematics*, 4(11), 1798–1813. <http://pvamu.edu/aam>.
- [13] Moitoi, A. J., & Shaw, S. (2023). Magnetic drug targeting during Caputo fractionalized blood flow through permeable vessel. *Microvascular Research*, 148, 104542. <https://doi.org/10.1016/j.mvr.2023.104542>.
- [14] Mohamed, N. A., Marei, I., Crovella, S., & Abou-Saleh, H. (2022). Recent developments in nanomaterials-based drug delivery and upgrading treatment of cardiovascular diseases. *International Journal of Molecular Sciences*, 23, 1403. <https://doi.org/10.3390/ijms23031404>.
- [15] Nguyen, M. D., Tran, H. V., Xu, S., & Lee, T. R. (2021). Fe_3O_4 nanoparticles: Structure, synthesis, magnetic properties, surface functionalization and emerging applications. *Applied Science*, 11(23), 11301.
- [16] Pan, D. C., Myerson, J. W., Brenner, J. S., Patel, P. N., Anselmo, A. C., Mitragotri, S., & Muzykantov, V. (2018). Nanoparticle properties modulate their attachment and effect on carrier red blood cells. *Scientific Reports*, 8, 1615, <https://doi.org/10.1038/s41598-018-1987-8>.
- [17] Pan, D., Vargas-Morales, O., Zern, B., Anseimo, A. C., Gupta, V., Zakrewsky, M., ... , Muzykantov, V. (2016). The effect of polymeric nanoparticles on bio-compatibility of carrier Red Blood Cells. *PLoS ONE*, 11, 3, e0152074. <https://doi.org/10.1371/journal.pone.0152074>.
- [18] Qiu, Y., Myers, D. R., & Lam, W. A. (2019). The biophysics and mechanics of blood from a materials prospective. *Nature Reviews Materials*, 4, 294–311. <https://doi.org/10.1038/s41578-019-0099-y>.

- [19] Qiu, L., Zhu, N., Feng, Y., Michaelides, E. E., Zyla, G., Jing, D., ..., Mahian, O. (2020). A review of recent advances in thermophysical properties of the nanoscale: from solid state to colloids. *Physics Reports*, 843, 1–81. <https://doi.org/10.1016/j.physrep.2019.12.001>.
- [20] Rao, L., Xu, J., Cai, B., Liu, H., Li, M., Jia, Y., ..., Zhao, X. (2016). Synthetic nanoparticles camouflaged with biomimetic erythrocyte membranes for reduced reticuloendothelial system uptake. *Nanotechnology*, 27, 085105.
- [21] Song, W., Jia, P., Zhang, T., Dou, K., Ren, Y., Liu, F., ..., Zhou, Q. (2022). Cell membrane-camouflaged inorganic nanoparticles for cancer therapy. *Journal of Nanobiotechnology*, 20, 289. <https://doi.org/10.1186/s12951-022-01475-w>.
- [22] Wang, S., Ma, S., Li, R., Qi, X., Han, K., Guo, L., & Li, X. (2023). Probing the interaction between supercarrier RBC membrane and nanoparticles for optimal drug delivery. *Journal of Molecular Biology*, 435, 167539. <https://doi.org/10.1016/j.jmb.2022.167539>.
- [23] Xia, Q., Zhang, Y., Li, Z., Hou, X., & Feng, N. (2019). Red blood cell membrane-camouflaged nanoparticles: A novel drug delivery system for antitumor application. *Acta Pharmaceutica Sinica B*, 9(4), 675–689. <https://doi.org/10.1016/j.apsb.2019.01.011>.
- [24] Yu, W., & Choi, S. U. S. (2003). The role of interfacial layers in the enhanced thermal conductivity of nanofluids: A renovated Maxwell model. *Journal of Nanoparticle Research*, 5, 167–171. <https://dx.doi.org/10.1023/A:1024438603801>.